8th ASME Symposium on Crashworthiness, Occupant Protection and Biomechanics in Transportation
November 14-19, 1999; Nashville, Tennessee,

Static and Dynamic Crush Testing and Analysis of a Rail Vehicle Corner Structural Element

Ronald A. Mayville, Randolph P. Hammond
Arthur D. Little, Inc.
Cambridge, Massachusetts 02140

Kent N. Johnson
Premiere Engineering Corp.
Atlanta, Georgia 30328

ABSTRACT

This paper presents the results of an experimental study to establish the strength and energy absorption capability of cab car rail vehicle corner structures built to current strength requirements and for structures modified to carry higher loads and absorb more energy. We reviewed current cab car structures and designed an end beam test element – the most common way of meeting current requirements – whose strength in the baseline state was at least 150,000 lbf. This design was then modified to provide a strength of over 400,000 lbf. The designs, which included consideration of the deformation and fracture response under impact loading, were carried out using conventional structural engineering methods and explicit finite element analysis.

INTRODUCTION

There is a relatively common type of train in the United States in which the lead car is a passenger vehicle with the operator sitting at the very front controlling either all of the individually-powered cars or the locomotive pushing at the other end. The operator sits within inches of the vehicle end in this cab car and is potentially susceptible to the damage that could occur in the event of a collision.

A number of train accidents over the last few years and recent research conducted under the direction of the Department of Transportation have demonstrated that the operator's corner of cab cars can be subjected to impacts that endanger crew and passengers. Figure 1 shows a photograph of the cab car struck by a locomotive in a switch in Secaucus, New Jersey in 1995 [1]. Other similar accidents have occurred in Silver Spring, Maryland also in 1995 [2] and Gary, Indiana in 1993 [3].

Figure 1: Photograph of the Cab Car Damaged in the Secaucus, New Jersey Accident [1].

Analyses have shown [4,5] that the collision speed at which dangerous crush of the cab car operator's volume occurs can be quite low – as low as 15mph for an offset collision with another train.

However, analyses have also demonstrated that the crashworthiness of cab cars subjected to offset collisions can be substantially improved with relatively modest increases in performance requirements. In particular, these studies have shown that the collision speed at which protection is provided to the operator can be increased by about 50% by ensuring that the corner structure can achieve a maximum load of 300,000 lbf with the ability to maintain this load for limited amounts of crush. This higher strength can be achieved by bringing the side sill forward to the corner post base. The added strength and energy absorption provided by this and other types of modifications are now being considered by the rail industry.

The work described in this paper was carried out to experimentally investigate the strength and energy absorption provided by cab car corner structures built to current industry standards and those that are modified to possess higher strengths with some energy absorption capability.

The results verify that substantially greater strength and energy absorption can be achieved with the addition of the side sill member and that the nonlinear finite element analysis provides good predictions of the response, provided accurate material data are used.

APPROACH

The approach to this project included design, fabrication, analysis and testing of cab car corner end beam structural elements with two strength levels. In one case, the structural element is intended to have a geometry and strength typical of that used in cab cars built to current U.S. structural specifications. In the second case this structural element was modified to achieve a substantially higher strength with the possibility of much greater energy absorption capability. In particular, the modification was made in a way that would be relatively easy to implement in new vehicle construction. Table 1 lists the tests conducted and the target end beam strengths.

Table 1: End Beam Tests Conducted

Test	Target End Beam Strength	Loading Method
1	150,000 lbf	Quasistatic
2	150,000 lbf	Dynamic
3	400,000 lbf	Dynamic

One test was conducted under quasistatic loading, since the corners of cab cars are currently designed under this assumption. We also wished to have test results for which the loading characteristics were accurately known so that good comparisons could be made to the companion finite element analysis.

The tasks undertaken in this program included a review of current cab car corner construction, design and fabrication of test articles and test fixtures, hand calculations and finite element analysis of the test articles and fixture, and testing.

REVIEW OF CAB CAR CONSTRUCTION

We reviewed the strength requirements and construction types for the corners of a number of cab cars currently in operation in the U.S. before generating the detailed design of the test article. Industry practice requires that the corner post have an ultimate strength of 150,000 lbf applied at the base along the axis of the car. The strict interpretation of this requirement is that only the corner post itself and

any reinforcement used need to possess the shear strength; the structure to which the post is attached need not. However, we understand that both the support structure and the post itself are generally designed to carry the 150,000 lbf load without failure. The corner post is also usually required to carry a load of about 30,000 lbf applied 18 inches above the floor without causing material yield.

In general, we found that cab cars, like most passenger cars operated in commuter service in the U.S., have an end underframe design similar to that schematically shown in Figure 2. The buff (end compression) load requirement, which for these vehicles is usually 800,000 lbf, is carried by the draft or center sill which runs down the center of the car. The corner post is usually supported at its base by a cantilever beam called the end beam or buffer wing. This type of construction is used to accommodate the stairwell that is normally located near all four corners of the vehicle. During cab operation, a plate drops down to provide the operator a place to stand.

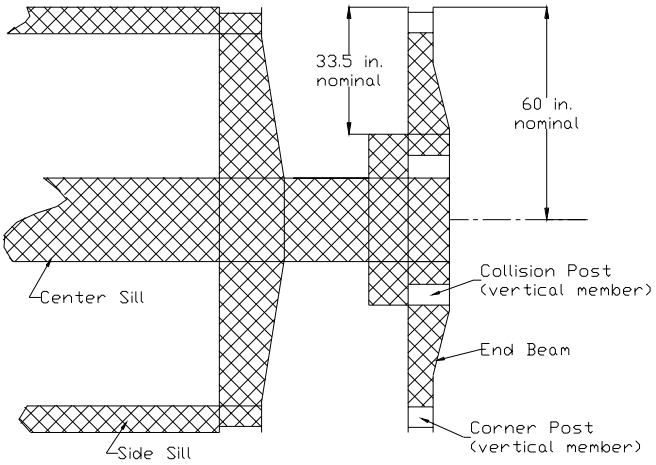

Figure 2: Typical End Underframe Design for Passenger Rail Vehicles Operated in Commuter Service in the U.S.

The T-shaped construction shown at the end of the underframe in Figure 2 is sometimes called the buffer sill and it often includes two rectangular holes which are used to anchor the collision posts that are located on each side of a doorway.

The ends of most U.S. commuter rail vehicles are constructed from high tensile structural steel having a yield strength of 50ksi. Welded construction is typical in the buffer sill.

TEST ARTICLE AND FIXTURE DESIGN

Test article design followed an iterative process in which hand calculations were accompanied by finite element analysis to arrive at the final design configurations. We present the final designs in this section and the analyses are summarized below.

Dimensions, materials and welding techniques representative of current U.S. rail car industry practice were used for the design and fabrication of the test articles. The resulting design, Figure 3, represents rail vehicle construction for the end beam and the adjacent structure. The design does not include a corner post because we were most interested in a loading that would be provided to the corner post support structure, such as would occur in a collision with another cab car or a locomotive. However,

the design does include a hollow rectangular section at the very end that could accommodate a corner post. The configuration also incorporates a hollow rectangular section in which a collision post could be accommodated. This is a very important detail because, as will be shown below, it is the location at which failure occurs in the tests.

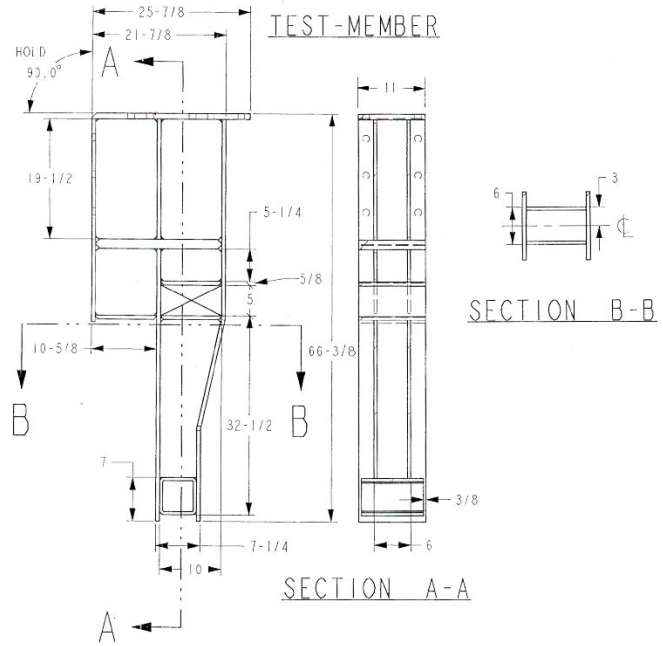

Figure 3: The Mechanical Drawing for the Baseline Test Article

Figure 4 shows the modified test article and the fixture used for both test article designs. A longitudinal member was added between the back of the corner post location and the end of the fixture. This member was intended to represent a strengthened side sill brought forward to the corner post. This 'side sill' member was welded to the test article and fixture using tubular lug reinforcements to eliminate the risk of connection fracture. We also added a transverse member to represent floor elements that would provide lateral support against buckling.

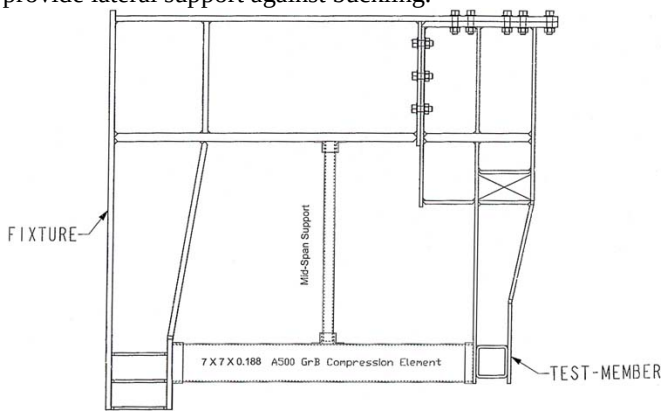

Figure 4: Modified Test Article Design with Fixture

MATERIALS AND PROPERTIES

A high-strength low alloy steel was used for the plate components of the end beam test article and fixture, with a few exceptions as noted below. Tensile specimens were machined from excess 0.50 in. thick plate supplied with the end beam/fixture materials. The specimens were machined in accordance with ASTM A370. Three specimens were cut parallel to and three specimens perpendicular to the rolling direction. Average properties from the tests are shown in Table 2.

Table 2: Measured Properties for the ASTM A572 Gr. 50 Used to Fabricate the Test Articles and Fixture

Yield Strength (lbf/in^2)	Tensile Strength (lbf/in^2)	Total Elongation (%)	Reduction of Area (%)
57,000	78,000	28	65

The material satisfied ASTM A572 Gr. 50. The 6 inch X 6 inch section used to represent the corner post lug was made from ASTM A500 Gr. B tube. (Property tests were not conducted for this material.)

The true-stress strain curve was derived from the engineering stress-strain curve and fit to the power-law relationship:

$\sigma = Ae^n$,

with A = 130 and n = 0.2 for stress in units of 10^3 lbf/in^2. The value of n = 0.2 is representative of the types of structural steels used to fabricate the test articles. The elastic constants used were, Young's Modulus = 29 X 10^6 lbf/in^2 and Poisson's Ratio = 0.29. These properties were used for all of the components in the analyses. Strain rate effects on the material properties were not considered in this project.

We considered a few fracture criteria for use in the finite element analysis. These included the elongation to fracture from the tension test and the following criterion:

$$e_f = \frac{e_t}{3(\frac{\sigma_m}{\sigma_e})}, \qquad (1)$$

where e_f = equivalent strain to fracture (general conditions)
e_t = true strain to fracture in a tension test
σ_m = mean stress (average of the principal stresses)
σ_e = equivalent or Mises stress.

The average true strain to fracture is derived from the tension test and for the A572 material is 1.05.

ANALYSIS

Baseline Test Article

The baseline test article was designed to have a corner post support strength of 150,000 lbf using conventional structural engineering techniques. Analysis revealed that the strength of an end beam

with the type of design shown in Figure 3 is determined by the strength of the plate element on the front side of the collision post opening.

The ultimate strength for a load applied at the corner post in the longitudinal direction is given approximately by:

$$F = (Area)(\sigma_{ult})\left(\frac{w}{h}\right) \qquad (2)$$

where $Area$ = the cross-sectional area of the plate element at the front of the collision post opening
σ_{ult} = the ultimate tensile strength
w = the depth of the end beam at the collision post opening
h = the distance from the collision post opening to the center of the corner post opening.

The strength calculated from equation (2) is 161,000 lbf. This value is close to and above the required strength value. However, the actual strength is much higher because the measured tensile strength, Table 2, is 78,000 lbf/in^2, 20% higher than the value assumed in design. Indeed, as shown in the section on testing, the measured strength was approximately 30% higher demonstrating the conservative nature of the common structural engineering approach used in most rail vehicle ultimate strength design.

Finite element analysis was conducted for both quasistatic and dynamic loading of the baseline test article to ensure that failure would occur in the components meant to represent the rail vehicle and to ensure that the test fixture would not be deformed or damaged in the static and dynamic tests.

A half-symmetrical finite element model of the baseline end beam and fixture was created using the commercially available ABAQUS® non-linear finite element computer programs (ABAQUS Standard to simulate the quasistatic loading and ABAQUS Explicit to simulate dynamic loading). A total of 2578 quad-plate elements and 2679 nodes comprised the half-symmetrical end beam / fixture model. The undeformed model is presented in Figure 5.

Loading was applied in the static case through a set of rigid elements meant to simulate the loading ram which had a radius of 3 inches. Contact friction was not included. The load was centered at a point of the end beam at the inner edge of the corner post opening (as opposed to the center of the opening as assumed in design.) This is the location of load application used in the tests. The rigid loading surface was constrained to follow the original line of loading without other translations or rotations.

A similar contact configuration was simulated in the dynamic analysis. Loading was applied by simulating a rigid mass (4,150 lbm to simulate actual test conditions, 40,000 lbm to obtain the overall load-crush response) traveling at a speed of 29 ft/sec (20 mph) at impact. This mass was also constrained against all motion except translation along the original path.

Figure 6 shows the load-deformation plot predicted for the baseline end beam configuration for both quasistatic and dynamic loading. Both analyses provide an end beam strength close to 240,000 lbf. This value is greater than the 161,000 lbf calculated using the specified minimum tensile strength for two reasons. First, the load in the analysis is applied three inches closer to the hinge point in the end beam. This results in a higher strength. When this moment arm factor is accounted for the strength calculated from the finite element analysis for a load centered in the corner post opening would be

216,000 lbf. This scaled value is 34% greater than the value calculated by hand. Most of this difference can be attributed to the higher actual tensile strength, 78,000 lbf/in^2, which is 20% greater than the 65,000 lbf/in^2 value assumed in the hand calculations. The rest of the difference is due to nonlinear effects not considered in the hand analysis such as the multiaxial deformation at the fracture location and the shortening of the moment arm with deformation.

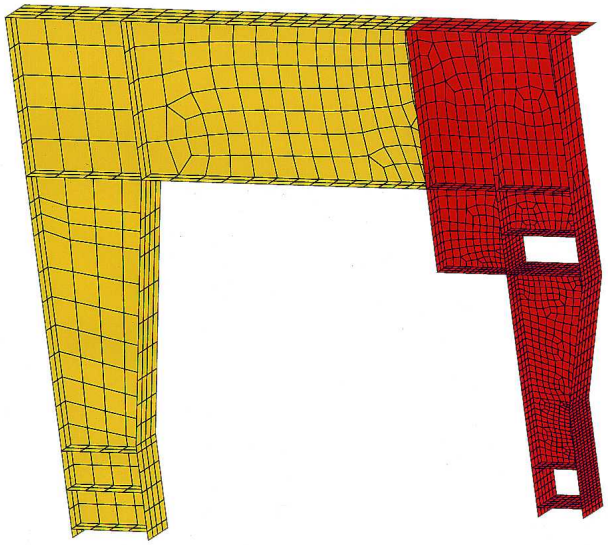

Figure 5: Half-Symmetrical End Beam / Fixture Finite Element Model

Fracture is predicted to occur (using the elongation criterion) at a corner displacement of about 6 inches in both cases with a total energy absorption of about 100x10^3 ft-lbf (135 kJ). The analysis also demonstrated that the fixture would not experience any significant plastic deformation or failure at connections. Load-crush predictions are compared to test results in the test section below. The predicted end beam displacement at fracture using the criterion (1) was 6.7 inches.

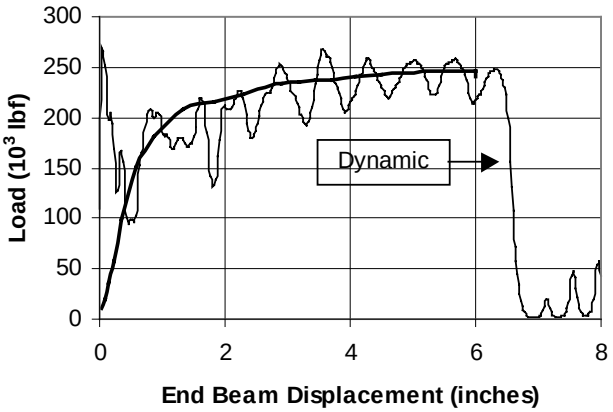

Figure 6: Predicted Load-Crush Responses for the Baseline End Beam Test Article Under Quasistatic and Dynamic Loading

Modified Test Article

The design of the supporting member for the modified test article was determined not only by the need to provide a higher peak strength but also to absorb energy through a regular folding pattern of deformation.

The cantilevered end beam and the supporting 'side sill' column can be considered to act in parallel to a first approximation. The required strength of the column is then (using the minimum strength approach):

F_{req} = 400,000 – 161,000 = 239,000 lbf.

The required cross-sectional area is then, assuming the column behaves as a compact element,

$A_{min} = F_{req}/\sigma_{yield}$ = 239,000/50,000 = 4.78 in^2.

The element chosen, Figure 4, has a cross-sectional area of 5.12 in^2 which gives a predicted total strength for the modified test article of 416,000 lbf.

A lateral support for the reinforcing 'side sill' member was added because the buckling stress was predicted to be less than the yield strength. Such a member can be thought to represent the support provided by floor and side members.

The crush load for the reinforcing member can be estimated from the approximate equations provided in [6], which, for a rectangular tube, give,

$$F_m = 5.2Ct\sigma_{yield}\left(\frac{4t}{C}\right)^{0.67}$$

where C = the outer dimension of the square tube and t = thickness. In our case with C = 7 inches, t = 0.188 inches, the predicted mean crush load is F_m = 77,000 lbf. This value was confirmed with separate finite element analysis on the column element.

The energy absorbed per unit crush for the column element is then, approximately,

E_{abs} = 77,000 ft-lbf/ft (340 kJ/m).

Higher energy absorption values could be obtained by selecting a column element with the same cross-sectional area but with a greater t/C ratio. We selected the 7x7x0.188 member to fit the dimensions of the test article and fixture.

The finite element analysis for the modified design was conducted using the same model as that used for the baseline geometry but modified to include the side sill supporting member. The model, after approximately two inches of simulated deformation, is shown in Figure 7; the predicted load-crush response is shown in Figure 8 compared to the dynamic response of the baseline end beam test article. The predicted peak load for the modified end beam is approximately 400,000 lbf. The corner displacement at which initial (end beam) failure is predicted was also 6 inches. However, in this case, the analysis predicts that the supporting 'side sill' member will still carry load and absorb energy. The total energy absorbed after 36 inches of crush is approximately 400,000 ft-lbf (540 kJ).

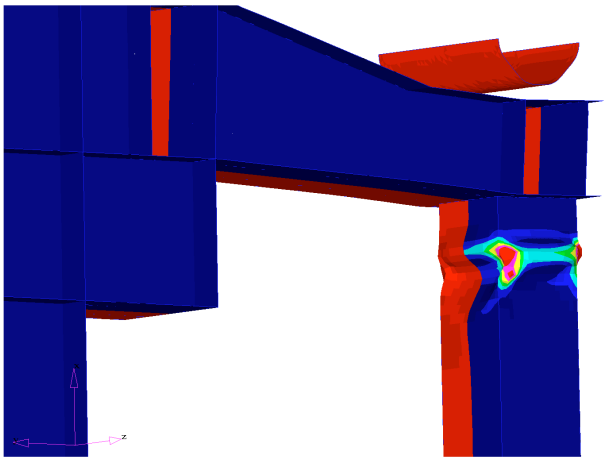

Figure 7: The Finite Element Model of Part of the Modified End Beam/Fixture After about Two Inches of Deformation

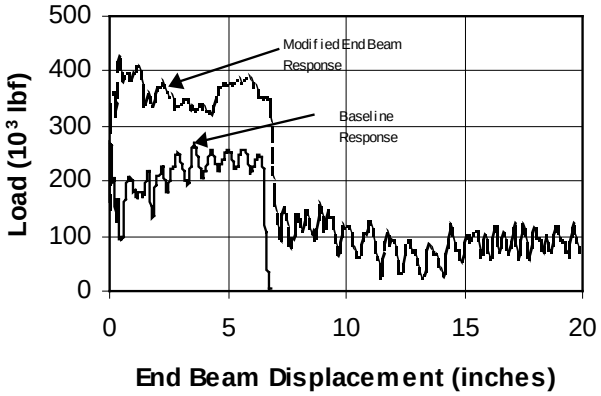

Figure 8: Dynamic Load-Crush Response Predicted for the Modified End Beam Test Article

TESTING

Testing included quasistatic loading of one of the baseline test articles and dynamic, drop tower testing of one baseline and one modified test article. Each test article was instrumented prior to testing with several strain gages. Testing was performed at the Transportation Sciences Center of Veridian/ Calspan in Buffalo, New York.

Quasistatic Testing

The crush machine used for quasistatic testing consists of a test bed, a fixed barrier, and a horizontally moving wall. The moving wall is driven by three, servo-controlled, hydraulic cylinders, each rated to a maximum total compressive force of 150,000 lbf and each in series with a load cell.

Figure 9 shows the baseline test article, the primary fixture and the loading fixture mounted in the quasistatic loading machine. The primary fixture was welded to the fixed wall and the loading fixture was welded to the moving wall and positioned to apply load in line with the inner surface of the corner post lug. The moving wall displacement rate was 1.25 inches/minute.

Results

Figure 10 shows the measured load-displacement curve from the quasistatic test. The figure also includes the predictions from the finite element analysis for comparison.

Figure 11 shows photographs of the test article after the test and, in particular, the location and form of fracture, which occurred in the plate element on the tension side of the collision post opening.

Figure 9: Quasi-Static Test Setup

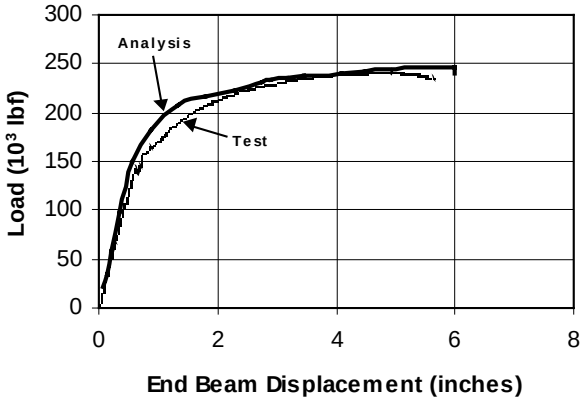

Figure 10: The Measured Load-Displacement Data from the Quasistatic Baseline End Beam Test Compared to the Finite Element Model Predictions

Measurements were made after the test of the total stretch at the location of failure. These data showed that the average longitudinal strain at fracture in the plate element that failed was approximately 0.28. This value is quite close to the average elongation to fracture in the tension test. The use of the multiaxial stress-dependent fracture criterion (1) predicts a stretch in the plate element at fracture of 0.35.

Figure 11: Close-Up Photographs of the Fracture Location in the Quasistatic, Baseline End Beam Test

Dynamic Testing

Dynamic testing was conducted using a drop tower facility for which the maximum drop height, above the test article, was approximately 12 ft and whose total drop mass was 4,150 lbm. This equates to an available energy of approximately 49,800 ft-lbf (68 kJ.) Because we expected both the baseline and modified test articles to absorb more energy than this we also anticipated the need for multiple drops on each test article.

The mass in the drop tower is guided to fall along a straight path by two adjacent parallel columns. In addition to strain gage instruments, the dynamic tests included two accelerometers mounted on the top of the mass (for use in deducing the load-time history on the test articles) and two high speed cameras. A computerized data acquisition system was used to record all data except that from the cameras. Data collection was triggered by a contact switch at the impact point on the end beam.

Baseline End Beam Test

The baseline end beam was subjected to two impacts from the drop tower for a total applied energy of about 100,000 ft-lbf (135 kJ). However, these impacts did not lead to fracture of the end beam. Instead, a substantial amount of deformation occurred in the drop tower guide columns, evidently because of the lateral load induced from the bending of the end beam. As a result, testing was ceased for this test article.

Figure 12 shows the measured load vs. time for the first drop. The experimental load was calculated as the product of the average acceleration (from the two accelerometers) and the drop mass. Although there are isolated, short-duration dynamic peaks, it is clear that the peak strength is approximately 240,000 lbf as was also measured in the quasistatic test for this configuration.

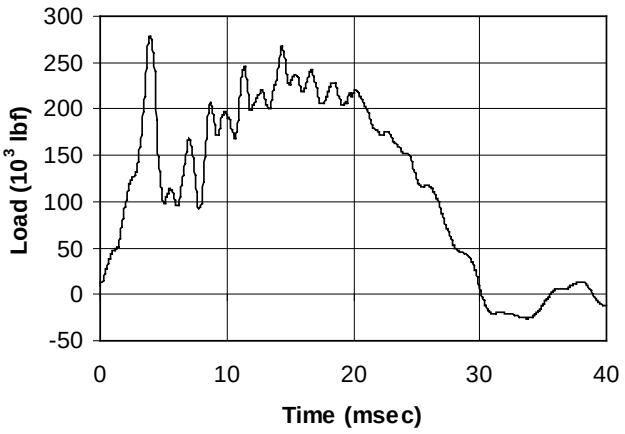

Figure 12: Measured Load (from Accelerometer Data)-Time Data from the First Impact on the Baseline End Beam Test Article

We observed in both impacts for this test article a rebound of the drop mass of about 1 ft. This indicates that the total energy delivered into plastic deformation of the test article/fixture assembly was actually about 45,500 ft-lbf (62 kJ) for each impact and 91,000 ft-lbf (123 kJ) for the two impacts combined. Additional deformation was observed in drop tower guide beams and the bolts used to connect the test fixture to the foundation, showing that the energy absorbed by the test article was even lower. This explains why fracture did not occur after the two impacts, since the total energy absorbed by the baseline end beam in the quasistatic test was approximately 96,000 ft-lbf (130 kJ). However, the agreement between calculations and measurements indicates that the baseline end beam will absorb the same amount of energy under static and dynamic loading conditions.

Modified End Beam Test

The modified end beam test article was also subjected to two impacts from the drop tower. We felt that the two impacts would provide enough data to confirm the primary requirements set out for this design and to confirm the ability of the finite element analysis to simulate the entire crush process.

Unfortunately, measurement system problems during both drops resulted in only a limited amount of data being available for our evaluation. The only reliable data available from the first impact is a measurement of permanent displacement of the end beam. Strains were available from the second impact. The values of the displacement for the two impacts on the modified end beam are shown in Table 3.

Table 3: Some of the Key Data Measured in the Dynamic, Modified End Beam Tests

Parameter	First Drop	Second Drop
End beam permanent displacement	0.80 inches	1.71 inches

Figure 13 shows the form of deformation at the top of the ‘side sill’ element after the first drop. We note that the folding type deformation desirable for energy absorbing elements has been initiated.

Our approach to estimating the ultimate strength for the modified end beam, which would have been exhibited for the first impact, is as follows.

a) Estimate the experimental load-time history for the second impact using the available elastic strain data and correlations between strain and load for the end beam elements
b) Modify the finite element analysis as needed to obtain agreement between the simulation and the available results, which are the end beam displacement data and the form of deformation for both impacts as well as the measured strains for the second impact
c) Use the predicted peak load from the analysis for the first impact as the measure of ultimate strength for the modified end beam test article.

The correlation between strain and load is made by assuming that the end beam and the ‘side-sill’ element act as parallel springs so that the force in each can be added. The strain-load correlation in the end beam is made by treating the end beam as a simple cantilever beam. The ‘side-sill’ element is assumed to act as a simple column in compression.

Figure 13: Photograph of the Modified End Beam at the Top of the ‘Side Sill’ Element after the First Impact

Figure 14 shows the strain-derived load vs. time plot for the second impact in comparison to the finite element analysis prediction and Table 4 compares the measured and finite element analysis predictions for the permanent displacement of the end beam end for the two impacts. These represent the optimized predictions. The finite element analysis used for these predictions includes all the assumptions previously described. (The only change that was necessary to obtain agreement between the strain-derived load and measured displacements and the finite element predictions was to use material strength values for the 'side sill' element that were the same as those used for the A572 Gr. 50 steel.)

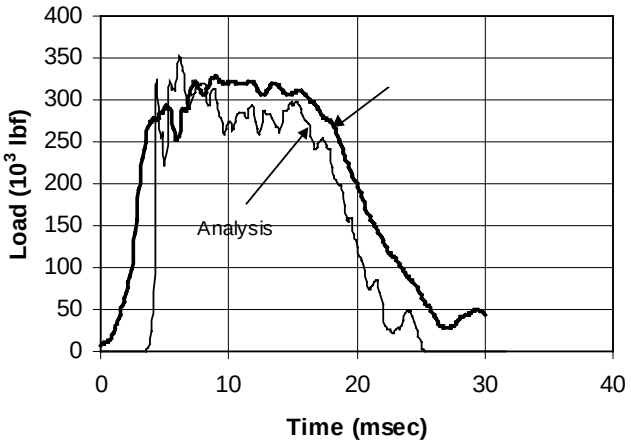

Figure 14: The Load-Time History for the Second Impact of the Modified End Beam Derived from Strain-Time Histories for the End Beam and 'Side Sill' Structural Elements with Comparison to the Finite Element Predictions

Table 4: Comparison of Measured and Predicted Load Displacements for the Modified End Beam Test Article

		Permanent Displacement from FEA (inches)
1	0.80	0.96
2	1.71	2.48

Finally, Figure 15 shows the load-time response predicted for the first impact by the optimized finite element analysis. We note that the predicted peak load is just over 400,000 lbf which matches the design goal. (Figure 8 showed the predicted load-crush response for a deformation of 20 inches.) A total energy absorption of 300,000 ft-lbf (410 kJ) is predicted at 20 inches of crush and, through extrapolation, we predict that 400,000 ft-lbf (540 kJ) would be absorbed after 36 inches of crush.

DISCUSSION

The results from this program have demonstrated a number of key points. It is clear that the conventional techniques used for ultimate strength design in rail vehicles can lead to very conservative results relative to the strength goals. Our baseline end beam was designed to have an ultimate strength of 150,000 lbf with some margin. The measured value was 240,000 lbf. This added strength comes

from material properties that were greater than the material minimum requirements and from material and geometric nonlinearities that were not considered in the hand calculations. There is no doubt that many of the rail vehicles currently on the road and designed to the 150,000 lbf strength value have substantially higher strengths and energy absorption potential. We have found such a difference for other rail vehicle structural components, such as the collision posts and anticlimbers on freight locomotives [7].

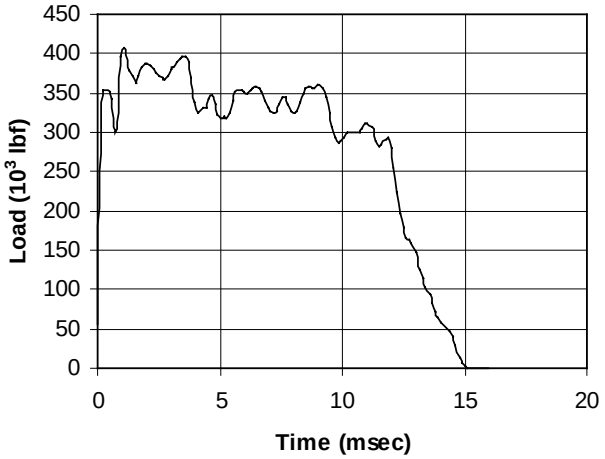

Figure 15: The Overall Predicted Load-Crush Response of the Modified End Beam Test Article

It is tempting to cite the disparity between the design goal and actual strength as an indication that the corner structures built to current standards provide more protection than we have calculated as possible in some of our previous studies [4,5,7]. However, this study demonstrates how the use of accurate material property data and finite element analysis techniques can enable a vehicle designer to potentially save weight and cost in meeting various structural requirements. Since the use of finite element analysis for ultimate strength design is becoming more widespread, we can expect the differences between design and actual strengths to become smaller in future. Therefore, it is necessary to specify the minimum crashworthiness requirements accurately.

This study has also shown how the addition of a relatively simple longitudinal member can substantially increase the strength and energy absorption capability of a cab car corner. In our study, this longitudinal member had a total weight of just 80 lbm.

The strength of the corner structure was increased to over 400,000 lbf and the energy absorption in one foot of crush was increased from 100,000 ft-lbf (135 kJ) to 250,000 ft-lbf (340 kJ). If the baseline design had just met the 150,000 lbf ultimate strength requirement the baseline energy absorption would have been approximately 63,000 ft-lbf (85 kJ) and the increase in energy absorption provided by the modified design would have been over a factor of three.

The potential increase in strength and energy absorption provided by the longitudinal member could have been, with some minor modifications, even greater than what we achieved. Our original hand calculations were based on the assumption that the peak strengths of the end beam cantilever member and the longitudinal column would be achieved simultaneously. However, it is clear that this does not

occur. Figure 10 showed that the peak strength of the cantilever end beam element is achieved only after about five inches of deformation, close to the point of fracture. On the other hand, the peak load in the compression element is achieved at much smaller displacements corresponding to the beginning of yielding of the column before the folding-type deformation initiates.

Figure 16 shows the computed contribution of only the compression element obtained by subtracting the load at a particular displacement for the baseline end beam from the total load at the same displacement for the modified end beam test article. The peak strength of the compression element, which is equal to about 260,000 lbf, occurs at a displacement of about 0.5 inches after which the load levels off to an average crush load of about 80,000 lbf, as predicted by hand calculations. Since the strength of the cantilever end beam element at 0.5 inches, Figure 10, is about 150,000 lbf, we obtain a total peak strength for the modified end beam of approximately 400,000 lbf.

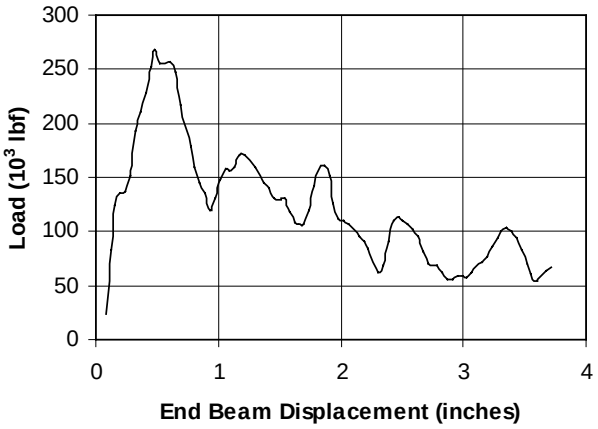

Figure 16: The Computed Contribution of the 'Side Sill' Compression Element in the Modified End Beam Test Article.

Thus, to obtain an even greater strength of the corner element we would need to increase the cross-sectional area or the yield strength of the 'side sill' element. For example, an increase in cross-sectional area to 7.5 in^2 for the same yield strength of 50,000 lbf/in^2 would increase the total modified end beam strength to about 550,000 lbf.

The other change that could be made to absorb more energy is to lower the *C/t* (side dimension-to-wall thickness) ratio for the 'side sill' element while maintaining approximately the same cross-sectional area. For example, a 5x5x5/16 inch steel square tube with a yield strength of 50,000 lbf/in^2 provides a slightly larger weight per unit length than the 7x7x3/16 inch tube used in our tests, but its average crush load is about 160,000 lbf compared to 80,000 lbf.

In summary, this study has demonstrated that the corners of cab cars can be modified to provide greater strength and energy absorption without substantial weight penalty. The study has also shown that nonlinear finite element analysis used with accurate material properties provides a very effective tool for determining the ultimate strength and energy absorption properties of rail vehicle structures under collision type loading.

ACKNOWLEDGEMENTS

This effort was conducted under contract to the Volpe National Transportation Systems Center, as part of the Equipment Safety Research Program sponsored by the Office of Research and Development of the Federal Railroad Administration. The authors would like to thank Ms. Kristine Severson and Mr. David Tyrell, of the Volpe Center for their helpful insight and direction.

REFERENCES

1. "Railroad Accident Report Near Head-on Collision and Derailment of Two New Jersey Transit Commuter Trains Near Seacaucus, New Jersey February 9, 1996," NTSB Report Number - RAR-97-01 , PB97-916301 (March 25, 1997) ..

2. "Collision and Derailment of Maryland Rail Commuter MARC Train 286 and National Railroad Passenger Corporation AMTRAK Train 29 Near Silver Spring, MD on February 16, 1996," NTSB Report Number - RAR-97-02 , PB97-916302 . (June 17, 1997)

3. "Collision Between Northern Indiana Commuter Transportation District Eastbound Train 7 and Westbound Train 12 Near Gary, Indiana on January 18, 1993," National Transportation Safety Board Railroad Accident Report. NTSB/RAR-93-03. PB93-916304. Washington, D.C. December 7, 1993.

4. Tyrell, D.C., Severson, K.J., Mayville, R.A., Stringfellow, R.G., Berry, S. and Perlman, A.B.,"Evaluation of Cab Car Crashworthiness Design Modifications," in Proceedings of the 1997 ASME/IEEE Joint Railroad Conference, March 18-20, 1997, Boston, Massachusetts (1997)49-58.

5. Stringfellow, R.G., Mayville, R.A., and Rancatore, R.J., "Evaluation of Protection Strategies for Cab Car Crashworthiness," to be published as a DOT-VNTSC-FRA Report, Cambridge, MA (1999).

6. Structural Impact, N. Jones (Cambridge, UK; Cambridge University Press) 1989

7. Mayville, R.A., *et al.*, *Locomotive Crashworthiness Research, Volumes 1-5* . DOT/FRA/ORD-95/08.1. DOT-VNTSC-FRA-95-4.1. Cambridge, MA. July 1995.